International Journal of Phytoremediation

ISSN: 1522-6514 (Print) 1549-7879 (Online) Journal homepage: www.tandfonline.com/journals/bijp20

Adsorptive potential of *Zea mays* tassel activated carbon towards the removal of metformin hydrochloride from pharmaceutical effluent

Menala Kalumpha, Upenyu Guyo, Ngceboyakwethu P. Zinyama, Felistus Muhle Vakira & Benias C. Nyamunda

To cite this article: Menala Kalumpha, Upenyu Guyo, Ngceboyakwethu P. Zinyama, Felistus Muhle Vakira & Benias C. Nyamunda (2020) Adsorptive potential of *Zea mays* tassel activated carbon towards the removal of metformin hydrochloride from pharmaceutical effluent, International Journal of Phytoremediation, 22:2, 148-156, DOI: 10.1080/15226514.2019.1652561

To link to this article: https://doi.org/10.1080/15226514.2019.1652561

View supplementary material

Published online: 19 Aug 2019.

Submit your article to this journal

Article views: 435

View related articles

View Crossmark data

Citing articles: 20 View citing articles

Full Terms & Conditions of access and use can be found at
https://www.tandfonline.com/action/journalInformation?journalCode=bijp20

INTERNATIONAL JOURNAL OF PHYTOREMEDIATION
2020, VOL. 22, NO. 2, 148–156
https://doi.org/10.1080/15226514.2019.1652561

Taylor & Francis
Taylor & Francis Group

Check for updates

Adsorptive potential of *Zea mays* tassel activated carbon towards the removal of metformin hydrochloride from pharmaceutical effluent

Menala Kalumpha[a,b], Upenyu Guyo[a], Ngceboyakwethu P. Zinyama[a], Felistus Muhle Vakira[b], and Benias C. Nyamunda[c]

[a]Department of Chemical Technology, Midlands State University, Senga, Zimbabwe; [b]Plus Five Pharmaceutical Pvt Ltd, Bulawayo, Zimbabwe; [c]Department of Chemical and Processing Engineering, Manicaland State University of Applied Sciences, Mutare, Zimbabwe

ABSTRACT

In the present study, *Zea mays* tassel which is a zero-value agricultural waste was used to produce a low-cost activated carbon using phosphoric acid as the activating agent. The prepared *Z. mays* tassel activated carbon (ZMTAC) was characterized by Fourier transform infrared spectroscopy (FTIR) and X-ray diffraction (XRD). The adsorbent was applied for adsorption of an emerging contaminant, metformin hydrochloride (MH) from pharmaceutical effluent. The effects of solution pH, contact time, adsorbent dosage, and initial MH concentration and their interactions were investigated using a response surface methodology following a central composite experimental design (CCD). The optimum experimental conditions were as follows: pH 9.5, contact time 67.50 min, dosage 0.5750 g, and MH concentration 152.50 mg/L. The isotherm data followed Langmuir isotherm model (R^2 = 0.979; sum of square deviation, SSD = 0.321). The saturation adsorption capacity of ZMTAC was 44.84 mg/g at 20 °C. MH adsorption process followed pseudo-second-order kinetics (higher R^2 and smaller SSD values). The thermodynamic properties obtained showed that the adsorption process was feasible, endothermic and spontaneous. Consequently, the study demonstrated that *Z. mays* tassel is a potential precursor for preparation of adsorbents for the removal of the MH from pharmaceutical effluent.

KEYWORDS

Zea mays tassel; activated carbon; metformin hydrochloride adsorption; isotherm; kinetics

Introduction

Pharmaceutical and Personal Care Products (PPCPs) are becoming a major source of contaminants that are posing a threat to humans, aquatic animals and the environment (Niemuth and Klaper 2015; Fakhri and Behrouz 2015a, 2015b). This is due to their incomplete metabolism in humans and their subsequent excretion as human waste thus finding their way in water through discharge in waste treatment plants (Fakhri and Khakpour 2015; Fakhri and Nejad 2016; Briones and Sarmah 2018).

Of all the PPCPs researched on, anti-diabetic drugs have received less attention. Current studies show that there is an increase in diabetic patients worldwide; hence, there is a need to determine their effects on release to the environment (Scheurer *et al.* 2012, 2009; Trautwein *et al.* 2014; Kosma *et al.* 2015; Huang *et al.* 2016; Tisler and Zwiener 2018). Metformin is one of the most prescribed anti-diabetic drugs for type 2 diabetes and is also considered as a potential drug for treatment of various cancers as well as endocrine disorders (Kosma *et al.* 2015; Bradley *et al.* 2016). It acts by primarily inhibiting complex 1 of the electron cellular chain impacting cellular balance and also increasing the cellular adenosine monophosphate: triphosphate ratio (Huang *et al.* 2016; Zhu *et al.* 2017). This results in inhibition of gluconeogenesis and activation of glycolysis and up-regulating glucokinase and fatty acid oxidation and also down regulating fatty acid synthase (Eggen *et al.* 2011).

Metformin (MET) is not metabolized by the human body thus is excreted in urine and in feces contributing to its high mass loads in wastewater treatment plants (WWTPs) (Briones and Sarmah 2018). Due to its high aqueous mobility and low K_{ow}, low molecular weight and high pKa, metformin persists in aqueous environments where it undergoes biodegradation into guanylurea (GUA) which is also persistent in aqueous environments (Briones and Sarmah 2018). MET and GUA are emerging as the greatest micropollutants due to their high prevalence in the soil and water environment (Bradley *et al.* 2016; Huang *et al.* 2016; Briones and Sarmah 2018) and potential endocrine disrupting effects. Metformin has been shown to be only biodegradable in the presence of specific and suitable degraders (Niemuth and Klaper 2015; Zhu *et al.* 2017). Metformin has been shown to impact negatively the growth of carrots if present in the soils in concentrations exceeding 10 mg/kg (Eggen *et al.* 2011). It is also reported to cause intersex gonads in male fish and affect the size of the same when exposed to 40 µg/L of metformin (Niemuth and Klaper 2015). Its presence in these

CONTACT Upenyu Guyo upguyo@gmail.com Department of Chemical Technology, Midlands State University, Private Bag 9055, Senga, Gweru, Zimbabwe
Supplemental data for this article can be accessed here.
Color versions of one or more of the figures in the article can be found online at www.tandfonline.com/bijp
© 2019 Taylor & Francis Group, LLC

environmental bodies poses a health and environmental threat to humans, animal, and plants. There is, therefore, a need to find ways of reducing their effects to human health and the ecosystem as a whole.

Of the conventional wastewater treatment methods, reverse osmosis, ozonation, advanced oxidation, and nanofiltration are the most effective (Huang *et al.* 2016; Zhu *et al.* 2017). However, due to the differences in hydrophilicity of PPCPs, some would require extra amount of energy which is costly. The removal of PPCPs predominantly occurs through degradation/transformation and adsorption (Briones and Sarmah 2018; Leone *et al.* 2018). Adsorption has been proved to be a suitable, efficient, and potential method due to its low cost, sorbent regeneration, diversified adsorption mechanisms, environmental benignity, and excellent adsorption performance. Various materials, raw or modified, have been employed in adsorption of various contaminants. These materials include ion exchange resins (Gupta *et al.* 2004), biochars (Tan *et al.* 2015, 2016, 2017; Bogusz *et al.* 2017; Yoon *et al.* 2017; Zhao *et al.* 2017), carbon nanotubes (Pyrzyńska and Bystrzejewski 2010; Yao *et al.* 2010; Ghaedi *et al.* 2012; Ghaedi and Kokhdan 2012; Ren *et al.* 2013, 2011), organic resins (Lu *et al.* 2016), biopolymers (Guyo, Matewere, Matina, Nharingo, *et al.* 2017a, Guyo, Matewere, Matina, Nyamunda, *et al.* 2017b), and graphene oxide (Zhu *et al.* 2017). Though these materials satisfactorily removed contaminants from various water sources, it is prudent to search for more low-cost higher performance materials.

Activated carbons (ACs) have been used widely in adsorption processes to remove numerous organic and inorganic contaminants from water bodies (Gu *et al.* 2009; Gedam and Dongre 2016). AC has an amorphous structure and is highly developed in pore size, pore volume and pore structure making it a highly efficient adsorbent (Gedam and Dongre 2016). In addition, AC also has numerous amounts of heteroatoms such as hydrogen, nitrogen, oxygen, phosphorous, and sulfur that exist as atoms bonded to the functional groups thus contributing to its unique adsorption properties. This also allows for surface modification to change its adsorption capacity and characteristics to suit a particular application.

The use of agricultural wastes as a source of activated carbon is becoming rampant as it helps in eradicating environmental pollution. Agricultural wastes are rich in cellulose, biodegradable, and non-meltable polymeric materials which are insoluble in most solvents due to hydrogen bonding and crystallinity (Kumar 2008; Sud *et al.* 2008). They have a number of functional groups which can bond either by physical or chemical adsorption as well as being rich in carbon content. However, natural cellulose has lower adsorption capacity as compared to modified cellulose thus its capacity can be enhanced to improve functionality and efficiency (Kumar 2008; Sud *et al.* 2008; Kumar *et al.* 2011; Oyelude and Appiah-takyi 2012) and also improve on surface area and pore volume.

The independent variables which affect adsorption efficiency, namely solution pH, adsorbent dosage concentration, solution temperature, contact time, and pollutant concentration, have been investigated and optimized using a Response surface methodology (RSM). A RSM is a mathematical statistical technique which optimizes the process and evaluates the relationship between a set of independent variables for specific responses with a minimum number of planned experiments (Fakhri *et al.* 2016). RSM evaluates the relative significance of the various independent variables in the presence of complex factor–factor interactions. Furthermore, a response surface (a graphical representation) is obtained which may describe the effects of the parameters on the response variable.

In the present study, *Zea mays* tassel which is a rich source of polymeric material and non-edible part of the *Z. mays* plant was chosen as a source of carbon. The tassels have desirable characteristics including binding functional groups (Moyo *et al.* 2013); hence, they are good precursors in the fabrication of novel adsorbents for remediation of pharmaceutical wastewaters. A RSM using a central composite design was used to optimize the adsorption process of metformin hydrochloride by *Z. mays* tassel derived adsorbent.

Materials and methods

Materials

All chemicals were used as received without further purification: Sodium hydroxide (Rochelle Chemicals, 98%), Phosphoric acid (ACE, 85%), Metformin Hydrochloride (Sino-bright, 100.29%), Hydrochloric acid (Rochelle Chemicals, 32%), and Distilled water (MSU laboratory).

Preparation of the Z. mays tassels

Zea mays tassels were outsourced from the City Council fields located in Bulawayo, Zimbabwe. The tassels were plucked off the main *Z. mays* plant, washed with 0.01 M HCl to remove any metals followed by distilled water, and oven dried at 105 °C for 24 h to remove moisture. The dried tassels were cut into small pieces, powdered in a grinding mill, sieved through a 150–250 µm mesh and stored in air-tight containers to avoid moisture build-up. The resulting sample was labeled ZMT.

Preparation of activated carbon

The activated carbon precursor, ZMT was initially carbonized in a muffle furnace at 300 °C before impregnation with 85% phosphoric acid (H_3PO_4) at an impregnation ratio of 1:4 (w/w) for 24 h. The impregnated material was filtered on a vacuum pump, dried at 105 °C for 12 h to get rid of moisture. Carbonization and chemical activation of the impregnated materials was carried out in a muffle furnace at 400 °C. The resultant activated material was allowed to cool for 1 h before sequential washing with hot and cold distilled water until the pH of the filtrate stabilized between 6 and 7. The resultant product was oven dried at 105 °C for 24 h and stored in an air-tight container prior to further use. The material was designated as ZMTAC.

Characterization of the adsorbent

The pH, loss of mass on ignition, moisture content, bulk density, acidity, and basicity of ZMTAC were determined using procedures reported elsewhere (Dada *et al.*, 2013; Nath *et al.*, 2013). The Fourier transform infrared spectroscopy (FTIR) spectra of ZMTAC were obtained using a Thermofischer Scientific spectrometer (Nicolet 6700, USA) in the scanning range 4000–400 cm^{-1}. A Bruker D8 Advance X-ray diffractometer (Germany) using nickel filtered Cu Kα radiation (40 kV, 40 mA) was used for identification of the structural phase.

Preparation of stock solution

A stock solution of 1000 mg/L of metformin dihydrochloride (MH) was prepared by dissolving approximately 1.00 mg of analytical grade MH in 100 mL of distilled water. The used concentrations were obtained by serial dilution of the stock solution.

Batch adsorption studies

Solution pH was adjusted to the desired value by using 0.1 M HCl and 0.1 M NaOH solutions. Adsorption studies were carried out by mixing appropriate amounts of adsorbent with 20 mL of metformin hydrochloride solution at a specified concentration. The mixture was agitated at 130 rpm using a dissolution tester (Pharma Test, PTWSIIIE, Germany) which has rotating paddles which aid interaction between the adsorbent and metformin hydrochloride for a specified time at room temperature. After agitation, the solid matrix was separated from the rest of the solution by filtration using Whatmann number 42 filter paper. The supernatant solution was analyzed for residual metformin hydrochloride (MH) using a Shimadzu UV 1800 UV-Vis spectrophotometer at 232 nm. The percentage removal (R) of MH from aqueous solution was determined using Equation (1):

$$R = \frac{(C_0 - C_e)}{C_0} \times 100\%. \quad (1)$$

The adsorption amount (q_e) was calculated according to the mass balance Equation (2):

$$q_e = \frac{(C_0 - C_e)V}{M}, \quad (2)$$

where q_e is the amount (mg/g) of MH adsorbed, C_0 and C_e are the MH concentrations (mg/L) in the solution initially and after adsorption, respectively, V is the volume (L) of the solution, and M is the mass (g) of ZMTAC used.

Experimental design

Batch adsorption studies were carried out following a central composite design (CCD) in the experimental domain shown in Table S1 (Supplementary data). Preliminary experiments were conducted to establish the levels of the independent variables shown in the experimental domain. Design Expert 11 trial version was used to optimize the process independent variables and evaluate their interactions (Mohammadi *et al.* 2016). MH adsorption efficiency (q_e) was taken as the response output variable. The quadratic model for the metformin hydrochloride (MH) adsorption process was proposed to be:

$$q_e = \beta_0 + \beta_1 A + \beta_2 B + \beta_3 C + \beta_4 D + \beta_5 A^2 + \beta_6 B^2 + \beta_7 C^2 + \beta_8 D^2 + \beta_9 AB + \beta_{10} AC + \beta_{11} AD + \beta_{12} BC + \beta_{13} BD + \beta_{14} CD. \quad (3)$$

where q_e is the adsorption capacity (mg/g), A is the pH, B is the contact time (min), C is the dosage (g), and D is the initial concentration (mg/L).

Adsorption–desorption studies

Adsorption–desorption studies were carried out in order to investigate on the potential to re-use the adsorbent. Desorption studies were carried out at optimum conditions after the optimization process was carried out for metformin hydrochloride desorption. Two sample bottles were labeled differently; a volume of 20 mL with concentration of 152.5 mg/L was placed in each sample bottle. The pH of the solutions was adjusted to 9.5 and a mass of 0.575 g of ZMTAC was added into each bottle. The bottles were agitated at 130 rpm for 67.5 min, and the samples were filtered using gravity filtration then taken for UV-VIS analysis. The adsorbent material was washed with 0.2 M HCl as a desorbing agent before it was thoroughly rinsed with distilled water and air dried. The adsorption-desorption process was repeated using the same adsorbent materials so as to obtain the number of cycles the adsorbent can be re-used. The obtained solutions were taken for UV-VIS analysis for determination of residual metformin hydrochloride.

Application on real effluent samples

The pharmaceutical effluent was sampled from a local Pharmaceutical Manufacturing Industry in Zimbabwe. The sample bottles were pretreated with detergent and thoroughly rinsed using distilled water. During sampling, it was made sure that the bottles were full in order to avoid the presence of air altering the sample chemically or biologically. The samples were analyzed on UV-Vis before and after adsorption of MH. The predetermined experimental conditions were applied to the real effluent samples.

Determination of sum of square deviation (SSD)

The best fit between the models was assessed by the SSD test which assumes that the model with the lowest SSD values best describes the sorption of MH onto ZMTAC. Equation (4) was used to calculate the SSD values:

$$SSD = \sum \left(\frac{(q_{t,e} - q_{t,m})}{q_{t,e}^2} \right)^2, \quad (4)$$

where $q_{t,e}$ and $q_{t,m}$ are the experimental adsorption capacities of MH in mg/g at time t, and the corresponding values obtained from the kinetic models, respectively.

Results and discussion

Characterization of ZMTAC

Physicochemical characteristics

Table S2 (Supplementary data) shows the physicochemical properties of ZMTAC such as bulk density, moisture content, pH_{ZPC}, surface area, ash content, and the Boehm's titration results. Small particle sizes (<180) means that the adsorbent had a larger surface area exposed to the adsorbate and hence enhanced removal of MH (Nharingo *et al.* 2015). The total ash content was 3.78% showing that the adsorbent was of high quality and hence could successfully remove MH from water sources (Moyo *et al.* 2015). The moisture content was significantly low (0.42%) showing that no dilution would be experienced during adsorption process. The bulk density was 0.48 g/mL indicating that ZMTAC materials had a large surface area for adsorption of MH. The results of the Boehm titrations show that ZMTAC had more acidic sites relative to basic sites implying that ZMTAC surface maintained acidic characteristics. The surface acidic and basic sites are responsible for adsorption of cationic and anionic species from water sources, respectively. Elemental composition analysis results (Supplementary data Table S2) show a significant amount of oxygen in the adsorbent confirming the presence of acidic functional groups such as the lactonic and carboxylic units on the surface of ZMTAC.

Fourier transform infrared (FTIR) spectroscopy

Figure 1a,b present the FT-IR spectra for ZMTAC before and after adsorption, respectively. The spectra vibrations of ZMTAC were analyzed before and after adsorption to determine the possible interactions between MH and the functional groups. The results showed that the activated carbon had different functional groups such as hydroxyl, carboxyl, and amide. The peaks at 3410.200 and 3228 cm^{-1} are due to N–H and OH stretching vibrations of polymeric compounds. Peaks at 1610.77 and 1400.86 cm^{-1} correspond to C = O stretching and N–H bending vibrations typical of carboxylate moieties and carboxylic groups, respectively (Moyo *et al.* 2015). The peaks observed at 2924.45 cm^{-1} and 2928.54 cm^{-1} are the stretching vibrations of C–H bands of carboxylic acids. The additional small peak at 1103.61 cm^{-1} indicates presence of S = O. A reduction, shift, or disappearance of peaks after adsorption suggests that interactions took place between the functional groups and the adsorbate. A significant shift in peaks (3410.20–3449.06 cm^{-1}; 1610.77–1635.28 cm^{-1}; 1400.86–1425.18 cm^{-1}; 1103.61–1083.17 cm^{-1}) suggested that interactions occurred between the functional groups and MH.

XRD analysis

Figure 1c presents the XRD pattern of activated carbon derived from *Z. mays* tassels. The spectrum shows a continuous function with partially resolved peaks at $2\theta = 22.6$ and 26.2 degrees, respectively, typical of an amorphous material.

Metformin hydrochloride adsorption response surface modeling

The experimental variables, experimental results, and predicted results obtained in MH adsorption following the 4-factors CCD matrix are presented in Table 1.

A proposed non-transformed second-order polynomial response equation (Equation (3)) which correlated dependent and independent variables was fitted on the experimental data obtained for the adsorption process. From the proposed Equation (3), insignificant terms ($p > 0.05$) were eliminated through step-wise regression analysis using Design Expert V11 and the regression results are presented in Table 2. From Table 2, the model terms B, C, D, AB, AC, BC, BD, B^2, C^2, and D^2 were significant ($p < 0.05$) (Fakhri 2014). The term, A, was retained in the model equation to support hierarchy.

Based on the regression results, the final model equation relating the response variable and the corresponding coded values (Supplementary data Table S5) was obtained and is

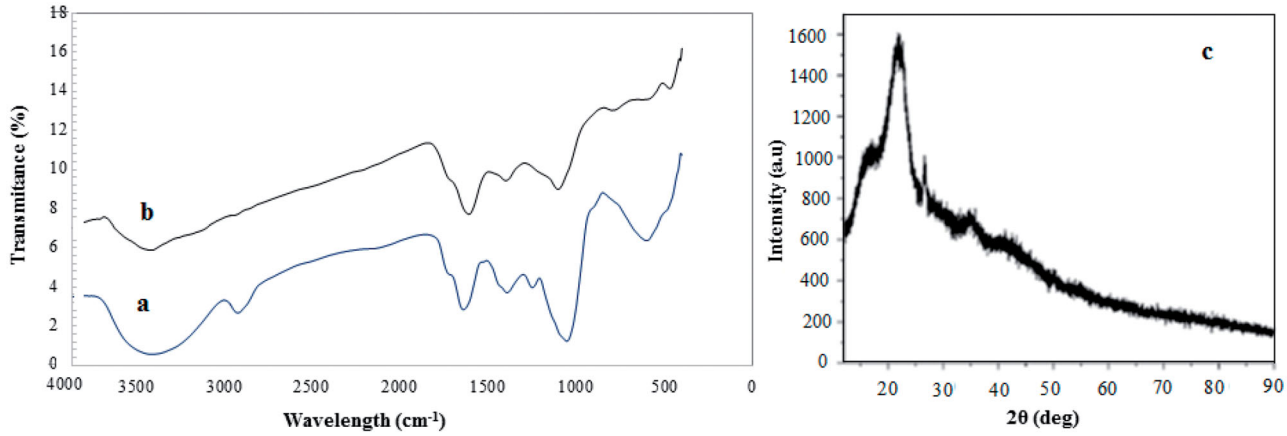


Figure 1. FTIR spectra of *Zea mays* tassel activated carbon before adsorption (a) and *Z. mays* tassel activated carbon after adsorption (b); XRD spectrum of *Z. mays* tassel activated (c).

Table 1 Experimental variables and results for MH adsorption using ZMTAC.

Run	Factor 1 pH	Factor 2 Contact time (min)	Factor 3 Dosage (g)	Factor 4 Concentration (mg/L)	Response q_e (mg/g)
1	7	125	1.05	105	1.4304
2	9.5	67.5	0.575	57.5	1.92
3	7	125	1.05	10	0.0895
4	9.5	182.5	0.575	57.5	1.8469
5	4.5	182.5	0.575	152.5	4.1043
6	4.5	67.5	1.525	57.5	0.7275
7	4.5	67.5	0.575	152.5	4.8838
8	7	125	1.05	105	1.1657
9	9.5	182.5	1.525	152.5	1.8715
10	4.5	182.5	1.525	152.5	1.9554
11	9.5	182.5	0.575	152.5	5.1009
12	4.5	67.5	0.575	57.5	1.8129
13	7	125	1.05	105	1.1836
14	7	125	0.1	105	9.984
15	7	125	1.05	105	0.9809
16	4.5	182.5	0.575	57.5	1.7997
17	12	125	1.05	105	0.8891
18	4.5	67.5	1.525	152.5	1.9321
19	9.5	67.5	1.525	57.5	0.4553
20	2	125	1.05	105	1.4242
21	9.5	67.5	0.575	152.5	2.704
22	7	10	1.05	105	1.6756
23	9.5	67.5	1.525	152.5	1.0331
24	4.5	182.5	1.525	57.5	0.3142
25	7	125	2	105	0.6118
26	7	240	1.05	105	0.3659
27	7	125	1.05	200	3.268
28	9.5	182.5	1.525	57.5	0.15
29	7	125	1.05	105	1.3259
30	7	125	1.05	105	1.3318

Table 2. ANOVA for response surface reduced quadratic model for MH using MTAC.

Source	Sum of squares	Mean square	*F*-value	*p*-Value	
Model	33.18	3.02	59.59	<0.0001	Significant
A-pH	0.0046	0.0046	0.0907	0.7678	
B-Contact time	1.30	1.30	25.71	0.0002	
C-Dosage	11.00	11.00	217.34	<0.0001	
D-Concentration	11.15	11.15	220.15	<0.0001	
AB	0.3996	0.3996	7.89	0.0139	
AC	0.6203	0.6203	12.25	0.0035	
BC	1.02	1.02	20.11	0.0005	
BD	1.02	1.02	20.06	0.0005	
B^2	1.15	1.15	22.78	0.0003	
C^2	1.39	1.39	27.50	0.0001	
D^2	0.3970	0.3970	7.84	0.0142	
Residual	0.7088	0.0506			
Lack of fit	0.5810	0.0646	2.53	0.1601	Not significant
Pure error	0.1278	0.0256			
Cor total	33.89				

presented using Equation (5).

$$q_e = 1.22 - 0.0150A + 0.3095B - 0.9148C + 0.7399D + 0.2827B^2 + 0.3194C^2 + 0.1212D^2 + 0.1764AB - 0.2218AC - 0.2841BC + 0.2813BD \quad (5)$$

Analysis of Variance (ANOVA) results for the regression process were used to evaluate the adequacy and significance of the quadratic model. A low *p*-value of less than 0.0001 and high *F*-value of 59.59 showed that the model was very significant (Montgomery *et al.* 2012; Cameron and Trivedi 2013). A higher regression model coefficient of determination ($R^2 = 0.9791$) further supports significance of the model as 97.91% variation in the observed data could be explained by the model. Furthermore, a small difference between adjusted R^2 and predicted R^2 (Supplementary data Table S6) of 0.0629 (<0.2) is further evidence supporting the significance of the model (Roosta *et al.* 2014). To further verify the adequacy of the model, a Lack of Fit test for the model which represents variance between the data and the fitted model was conducted. If the model does not sufficiently fit the data, then the Lack of Fit *p*-value will be less than 0.05. Based on the ANOVA results, the Lack of Fit *p*-value obtained for this model was 0.1601 (Table 2) which is greater 0.05 showing that is was insignificant and hence the model was capable of interpreting the adsorption data. To add to this, an adequate precision (measures the signal-to-noise ratio) greater than 4 is desirable. In this analysis, an adequate precision of 31.9490 (Table S6) was obtained showing an adequate signal.

The model was also evaluated graphically for its adequacy and validity. Normal probability plot was used to check for normality of data from the quadratic model. From Figure S3a (Supplementary data), it can be seen that the residuals lie along the oblique straight line with no apparent pattern showing that the data was normally distributed. Figure S3b (Supplementary data) shows a plot of standard residuals versus the predicted response. For a valid model, the residuals should be randomly scattered around the zero line showing that the data is not reflecting an abnormal behavior as presented in Figure S3b (Supplementary data). Again from Figure S3b (Supplementary data), it can be seen that there are no outliers (residuals outside the red lines). Figure S3c (Supplementary data) shows a plot of experimental data versus predicted data. There should be a strong agreement between these as evidenced by the data points falling on or being close to the oblique line. This shows that the model best represented the experimental data.

Effects of variables as response surface plots

To investigate the influence of the independent variables (pH, adsorbent dosage, contact time, and MH concentration) on adsorption of MH onto ZMTAC, the three dimensional surface plot are presented in Figure 2. Figure 2a presents the combined influence of solute pH and contact time on adsorption capacity, q_e. From Figure 2a, it is apparent that pH has no significant effect on adsorption capacity, q_e, though it has a small negative effect. This means that an increase in pH results in a slight decrease in adsorption capacity attributed to the changes in surface functionalities on the adsorbent and MH as a result of variances in pH. An increase in contact time increased q_e due to the elongated time of interaction between the metformin hydrochloride ions and the adsorbent active sites. Figure 2b illustrates the combined influence of solute pH and dosage on q_e. Again, pH profile shows no apparent influence on q_e as explained earlier on. An increase in adsorbent dosage is shown to decrease q_e. This may be perhaps due to overlap of adsorption sites as the adsorbent concentration is increased.

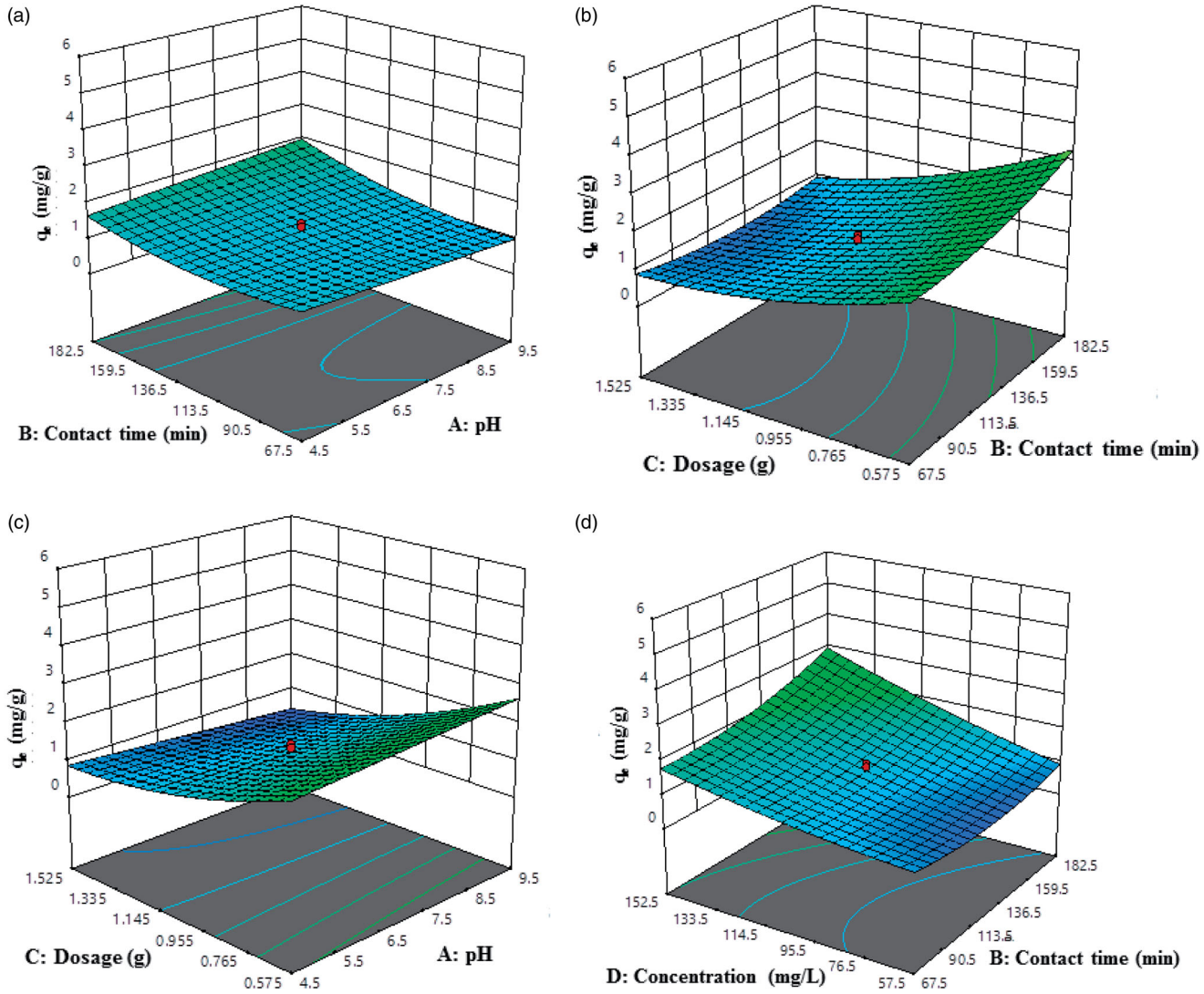


Figure 2. 3D surface plot for the combined effect of pH and contact time (a), contact time and dosage (b), pH and dosage (c), and contact time and concentration (d) on Cd(II) adsorption efficiency.

Figure 2c illustrates the interactive effect of contact time and adsorbent dosage on *qe*. From Figure 2c, it is clear that increasing both contact time and dosage results in a decrease in q_e. Figure 2d shows that increasing MH concentration and contact time increases adsorption capacity.

Optimization of MH adsorption process

Numerical optimization of the adsorption process was conducted using the desirability function on the Design Expert software. The criterion used was such that pH be in the range 4.5–9.5, contact time be minimum, dosage be minimum, and MH concentration be maximum. The optimum experimental conditions were determined to be pH 9.5, contact time (67.50 min), dosage (0.5750 g), and MH concentration (152.50 mg/L).

Adsorption kinetics

The mechanism of the adsorption process was determined using the pseudo-first-order (Lagergren 1898) and pseudo-second-order (Ho and McKay 1999) models.

The kinetic models (Supplementary data Figure S5) were expressed in linear forms as shown in Equations (6) and (7):

$$\text{Pseudo}-\text{first}-\text{order}: \ \log\left(q_e - q_t\right) = \log q_e - \frac{t.\ k_1}{2.3} \tag{6}$$

$$\text{Pseudo}-\text{second}-\text{order}: \ \frac{t}{q_t} = \frac{t}{q_e} + \frac{1}{k_2(q_e)^2}, \tag{7}$$

where, q_e and q_t are the amount of MH adsorbed (mg/g) onto ZMTAC at equilibrium and at any time t, respectively, t is the time (min) and k_1 (min^{-1}) and k_2 (g/mg/min) are the equilibrium rate constants of pseudo-first-order and pseudo-seconds order models, respectively.

The pseudo-second-order kinetic model had a correlation coefficient of 0.996 as compared to 0.949 for the pseudo-second order model (Supplementary data Table S7). This evidence together with lower SSE value (0.0412 for second order versus 0.896 for first order) and better agreement between $q_{e,cal}$ value (0.925 mg/g for second order versus 3.023 mg/g for first order) and $q_{e,exp}$ value (1.03 mg/g) supports the suitability of the pseudo-second-order model to

the adsorption of MH. The adsorption of MH onto ZMTAC was hence concentration depended and the rate determining step involved chemical adsorption.

Adsorption isotherms

Freundlich (1906) and the Langmuir (1916) adsorption isotherms were used to interpret the by varying experimental data. The models are represented in linear forms as follows:

$$\text{Langmuir isotherm}: \quad \frac{1}{q_e} = \frac{1}{q_{max}} + \left(\frac{1}{bq_{max}}\right)\frac{1}{C_e} \tag{8}$$

$$\text{Freundlich isotherm}: \quad \ln q_e = \ln K_F + \frac{1}{n}\ln C_e, \tag{9}$$

where q_e is the amount of MH adsorbed at equilibrium, q_m is the maximum adsorption capacity (mg/g), C_e (mg/L) is the equilibrium concentration, and K_L is the Langmuir sorption constant (L/mg) related with the free energy of sorption, K_F (mg/g) and n are constants representing the adsorption capacity and intensity of adsorption, respectively.

The linear model plots are presented in Figure S6 (Supplementary data). The coefficients of determination (0.979 for Langmuir model versus 0.943 for Freundlich model) together with the sum of square errors (0.321 for Langmuir model versus 2.987 for Freundlich model) show that the Langmuir model sufficiently described the relationship between q_e and C_e. The summary of the models parameters is presented in Table S8 (Supplementary data).

Adsorption thermodynamics

The thermodynamic nature of the adsorption process was determined by carrying out experimental adsorption temperature whilst maintaining the other independent variables constant. This was followed by estimating thermodynamic parameters such as standard Gibb's free energy change (ΔG^o), the entropy change (ΔS^o) and the enthalpy change (ΔH^o) from Equations (10) to (13):

$$\Delta G^o = -RT\ln K_d \tag{10}$$

$$K_d = \frac{q_e}{C_e} \tag{11}$$

$$\Delta G^o = \Delta H^o - T\Delta S^o \tag{12}$$

$$\ln K_d = \frac{\Delta S^o}{R} - \frac{\Delta H^o}{RT}, \tag{13}$$

where R is the ideal gas constant, T is the temperature in K, and K_d is the thermodynamic equilibrium constant. The parameter, q_e is the amount of MH adsorbed at equilibrium in mg/L, and C_e is the equilibrium concentration of MH in solution. The standard Gibbs free energy change (ΔG^o) values (Supplementary data Table S9) were found to be −5.79, −6.09, and −6.68 kJ/mol at 298.15, 308.15, and 328.15 K, respectively, providing evidence for the feasibility and spontaneity of the adsorption process. The adsorption process was also endothermic reflecting randomness at the solid/solution interface as evidenced by the positive ΔH^o (+3.096 kJ/mol) and ΔS^o (+0.0298 kJ/mol). The low ΔH^o value and the less negative ΔG^o values are characteristic of a physical adsorption process.

Adsorption–desorption studies

Repeated adsorption–desorption studies were conducted to investigate regeneration and reusability of ZMTAC loaded with MH. Even after 6 adsorption–desorption cycles, 81.5% (Supplementary data Figure S7) of MH could still be removed from synthetic MH aqueous solutions. This is evident that ZMTAC can be reused several times in remediation of MH contaminated waters.

Application on real effluent samples

ZMTAC was evaluated for its practical applicability on remediation of wastewaters. Real pharmaceutical effluent sample was collected from a local Pharmaceutical Manufacturing Company. The effluent sample was analyzed for the presence and concentration levels of MH prior to an adsorption process using the optimized experimental conditions. A removal efficiency of 94.19% was recorded showing that ZMTAC is a potential candidate for remediation of MH contaminated waters.

Conclusions

The study explored the use of ZMTAC as a potential adsorbent in the removal of metformin hydrochloride from wastewaters. The effects of pH, contact time, adsorbent dosage, and initial concentration on MH adsorption were investigated using a response surface methodology (RSM). These independent variables were optimized numerically using the desirability function and the optimum experimental conditions were determined to be pH 9.5, contact time (67.70 min), dosage (0.5750 g), and MH concentration (152.50 mg/L). The kinetic and isotherm behaviors of the adsorption process were best by pseudo-second-order model and Langmuir model, respectively. The adsorption process was spontaneous and endothermic as confirmed by the thermodynamic studies. MZTAC showed excellent adsorption capacity after several adsorption–desorption cycles implying that it can be regenerated. Physical and chemical interactions between the adsorbent and MH were both shown to be present. The present study demonstrated that ZMTAC could be an efficient adsorbent for MH as evidenced by a 94% MH removal from real life effluent samples.

Funding

The authors would like to thank Midlands State University Research Board for funding the research.

References

Bogusz A, Nowak K, Stefaniuk M, Dobrowolski R, Oleszczuk P. 2017. Synthesis of biochar from residues after biogas production with respect to cadmium and nickel removal from wastewater. J Environ Manage. 201:268–276. doi:10.1016/j.jenvman.2017.06.019.

Bradley PM, Journey C. A, Button DT, Carlisle DM, Clark JM, Mahler BJ, Nakagaki N, Qi SL, Waite IR, VanMetre PC. 2016. Metformin and other pharmaceuticals widespread in wadeable streams of the southeastern United States. Environ Sci Technol Lett. 3(6):243–249. doi:10.1021/acs.estlett.6b00170.

Briones RM, Sarmah AK. 2018. Detailed sorption characteristics of the anti-diabetic drug metformin and its transformation product guanylurea in agricultural soils. Sci Total Environ. 630:1258–1268. doi:10.1016/j.scitotenv.2018.02.306.

Cameron A, Trivedi P. 2013. Regression analysis of count data. Cambridge: Cambridge University Press.

Dada AO, Ojediran JO, Olalekan AP. 2013. Sorption of Pb^{2+} from aqueous solution unto modified rice husk: isotherms studies. Adv Phys Chem. 2013:1. doi:10.1155/2013/842425.

Eggen T, Normann T, Grave K, Hormazabal V. 2011. Uptake and translocation of metformin, ciprofloxacin and narasin in forage- and crop plants. Chemosphere. 85(1):26–33. doi:10.1016/j.chemosphere.2011.06.041.

Fakhri A. 2014. Application of response surface methodology to optimize the process variables for fluoride ion removal using maghemite nanoparticles. J Saudi Chem Soc. 18(4):340–347. 3, doi:10.1016/j.jscs.2013.10.010.

Fakhri A, Behrouz S. 2015a. Photocatalytic properties of tungsten trioxide (WO_3) nanoparticles for degradation of Lidocaine under visible and sunlight irradiation. Sol Energy. 112:163–168. doi:10.1016/j.solener.2014.11.014.

Fakhri A, Behrouz S. 2015b. Assessment of S_nS_2 nanoparticles properties for photocatalytic and antibacterial applications. Sol Energy. 117:187–191. doi:10.1016/j.solener.2015.04.016.

Fakhri A, Khakpour R. 2015. Synthesis and characterization of carbon or/and boron-doped CdS nanoparticles and investigation of optical and photoluminescence properties. J Lumin. 160:233–237. doi:10.1016/j.jlumin.2014.12.019.

Fakhri A, Nejad PA. 2016. Antimicrobial, antioxidant and cytotoxic effect of molybdenum trioxide nanoparticles and application of this for degradation of ketamine under different light illumination. J Photochem Photobiol B: Biol. 159:211–217. doi:10.1016/j.jphotobiol.2016.04.002.

Fakhri A, Rashidi S, Tyagi I, Agarwal S, Gupta VK. 2016. Photodegradation of erythromycin antibiotic by γ-Fe_2O_3/SiO_2 nanocomposite: response surface methodology modeling and optimization. J Mol Liquids. 214:378–383. doi:10.1016/j.molliq.2015.11.037.

Freundlich HM. 1906. Over the adsorption in solution. J Phys Chem. 57:384–470.

Gedam AH, Dongre RS. 2016. Activated carbon from *Luffa cylindrica* doped chitosan for mitigation of lead(ii) from an aqueous solution. RSC Adv. 6(27):22639–22652. doi:10.1039/C5RA22580A.

Ghaedi M, Khajehsharifi H, Yadkuri AH, Roosta M, Asghari A. 2012. Oxidized multiwalled carbon nanotubes as efficient adsorbent for bromothymol blue. Toxicol Environ Chem. 94(5):873–883. doi:10.1080/02772248.2012.678999.

Ghaedi M, Kokhdan S. 2012. Oxidized multiwalled carbon nanotubes for the removal of methyl red (MR): kinetics and equilibrium study. Desalin Water Treat. 49(1-3):317–325. doi:10.1080/19443994.2012.719355.

Gu W, Sun CJ, Liu Q, Cui HX. 2009. Adsorption of avermectins on activated carbon: Equilibrium, kinetics, and UV-shielding. Trans Nonferrous Met Soc China (English Ed). 19:s845–s850. doi:10.1016/S1003-6326(10)60163-X.

Gupta VK, Singh P, Rahman N. 2004. Adsorption behavior of Hg(II), Pb(II), and Cd(II) from aqueous solution on Duolite C-433: a synthetic resin. J Colloid Interface Sci. 275(2):398–402. doi:10.1016/j.jcis.2004.02.046.

Guyo U, Matewere N, Matina K, Nharingo T, Moyo M. 2017a. Fabrication of a sustainable maize stover-graft-methyl methacrylate biopolymer for remediation of methyl red contaminated wasters. Sustain Mater Technol. 13:9–17. doi:10.1016/j.susmat.2017.05.001.

Guyo U, Matewere N, Matina K, Nyamunda BC, Moyo M. 2017b. Preparation of poly(methyl methacrylate)–grafted *Hyparrhenia hirta* for methyl red removal from colored solutions. Bioremediat J. 21(3–4):163–175. doi:10.1080/10889868.2017.1337710.

Ho Y, McKay G. 1999. Pseudo second order model for sorption processes. Process Biochem. 34(5):451–465. doi:10.1016/S0032-9592(98)00112-5.

Huang X, Liu Y, Liu S, Li Z, Tan X, Ding Y, Zeng G, Xu Y, Zeng W, Zheng B. 2016. Removal of metformin hydrochloride by: *Alternanthera philoxeroides* biomass derived porous carbon materials treated with hydrogen peroxide. RSC Adv. 6(83):79275–79284. doi:10.1039/C6RA08365J.

Kosma CI, Lambropoulou D. A, Albanis T. A. 2015. Comprehensive study of the antidiabetic drug metformin and its transformation product guanylurea in Greek wastewaters. Water Res. 70:436–448. doi:10.1016/j.watres.2014.12.010.

Kumar PS, Ramalingam S, Kirupha SD, Murugesan A, Vidhyadevi T, Sivanesan S. 2011. Adsorption behavior of nickel(II) onto cashew nut shell: equilibrium, thermodynamics, kinetics, mechanism and process design. Chem Eng J. 167(1):122–131. doi:10.1016/j.cej.2010.12.010.

Kumar U. 2008. Agricultural products and by-products as a low cost adsorbent for heavy metal removal from water and wastewater: a review. Sci Res Essay. 1:33–37.

Lagergren S. 1898. About the theory of so-called adsorption of soluble substances. K. Sven Vetenskapsakademiens Handl. 24:1–39.

Langmuir I. 1916. The constitution and fundamental properties of solids and liquids-part 1: solids. J Am Chem Soc. 38(11):2221–2295. doi:10.1021/ja02268a002.

Leone VO, Pereira MC, Aquino SF, Oliveira LCA, Correa S, Ramalho TC, Gurgel LV. A, Silva AC. 2018. Adsorption of diclofenac on a magnetic adsorbent based on maghemite: experimental and theoretical studies. New J Chem. 42(1):437–449. doi:10.1039/C7NJ03214E.

Lu X, Shao Y, Gao N, Chen J, Zhang Y, Wang Q, Lu Y. 2016. Adsorption and removal of clofibric acid and diclofenac from water with MIEX resin. Chemosphere. 161:400–411. doi:10.1016/j.chemosphere.2016.07.025.

Mohammadi S, Sohrabi M, Golikand AN, Fakhri A. 2016. Preparation and characterization of zinc and copper co-doped WO_3 nanoparticles: application in photocatalysis and photobiology. J Photochem Photobiol B Biol. 161:217–221. doi:10.1016/j.jphotobiol.2016.05.020.

Montgomery D, Peck E, Vining G. 2012. Introduction to linear regression analysis. New York, NY: John Wiley & Sons.

Moyo M, Chikazaza L, Nyamunda BC, Guyo U. 2013. Adsorption batch studies on the removal of Pb(II) using maize tassel based activated carbon. J Chem. 2013:1–8. doi: 10.1155/2013/508934.

Moyo M, Sikwila TL, Sebata E, Nyamunda BC, Guyo U. 2015. Equilibrium, kinetic, and thermodynamic studies on biosorption of Cd (II) from aqueous solution by biochar. Res Chem Intermed. 42(2):1349–1362. doi:10.1007/s11164-015-2089-z

Nath K, Panchani S, Bhakhar MS, Chatrola S. 2013. Preparation of activated carbon from dried pods of *Prosopis cineraria* with zinc chloride activation for the removal of phenol. Environ Sci Pollut Res. 20(6):4030–4045. doi:10.1007/s11356-012-1325-y.

Nharingo T, Ziwurawa M, Guyo U. 2015. Exploring the use of cactus *Opuntia ficus indica* in the biocoagulation–flocculation of Pb(II) ions from wastewaters. J Environ Sci Technol. 12:3791–3802. doi:10.1007/s13762-015-0815-0.

Niemuth NJ, Klaper RD. 2015. Emerging wastewater contaminant metformin causes intersex and reduced fecundity in fish. Chemosphere. 135:38–45. doi:10.1016/j.chemosphere.2015.03.060.

Oyelude EO, Appiah-Takyi F. 2012. Removal of methylene blue from aqueous solution using alkali-modified malted sorghum mash. Turkish J Eng Environ Sci. 36:161–169. doi:10.3906/muh-1108-6

Pyrzyńska K, Bystrzejewski M. 2010. Comparative study of heavy metal ions sorption onto activated carbon, carbon nanotubes, and carbon-

encapsulated magnetic nanoparticles. Colloids Surfaces A Physicochem Eng Asp. 362(1-3):102–109. doi:10.1016/j.colsurfa.2010.03.047.

Ren X, Chen C, Nagatsu M, Wang X. 2011. Carbon nanotubes as adsorbents in environmental pollution management: a review. Chem Eng J. 170(2-3):395–410. doi:10.1016/j.cej.2010.08.045.

Ren X, Li J, Tan X, Wang X. 2013. Comparative study of graphene oxide, activated carbon and carbon nanotubes as adsorbents for copper decontamination. Dalton Trans. 42(15):5266–5274. doi:10.1039/c3dt32969k.

Roosta M, Ghaedi M, Daneshfar A, Sahraei R. 2014. Experimental design based response surface methodology optimization of ultrasonic assisted adsorption of safaranin O by tin sulfide nanoparticle loaded on activated carbon. Spectrochim ACTA A Mol Biomol Spectrosc. 122:223–231. doi:10.1016/j.saa.2013.10.116.

Scheurer M, Michel A, Brauch HJ, Ruck W, Sacher F. 2012. Occurrence and fate of the antidiabetic drug metformin and its metabolite guanylurea in the environment and during drinking water treatment. Water Res. 46(15):4790–4802. doi:10.1016/j.watres.2012.06.019.

Scheurer M, Sacher F, Brauch HJ. 2009. Occurrence of the antidiabetic drug metformin in sewage and surface waters in Germany. J Environ Monit. 11(9):1608–1613. doi:10.1039/b909311g.

Sud D, Mahajan G, Kaur MP. 2008. Agricultural waste material for sequestering heavy metals ions from aqueous solutions: a review. Bioresour Technol. 99(14):6017–6027. doi:10.1016/j.biortech.2007.11.064.

Tan X, Liu S, Liu Y, Gu Y, Zeng G, Hu X, Wang X, Liu S, Jiang L. 2017. Biochar as potential sustainable precursors for activated carbon production: multiple applications in environmental protection and energy storage. Bioresour Technol. 227:359–372. doi:10.1016/j.biortech.2016.12.083.

Tan X, Liu Y, Zeng G, Wang X, Hu X, Gu Y, Yang Z. 2015. Application of biochar for the removal of pollutants from aqueous solutions. Chemosphere. 125:70–85. doi:10.1016/j.chemosphere.2014.12.058.

Tan XF, Liu YG, Gu YL, Xu Y, Zeng GM, Hu XJ, Liu SB, Wang X, Liu SM, Li J. 2016. Biochar-based nano-composites for the decontamination of wastewater: a review. Bioresour Technol. 212:318–333. doi:10.1016/j.biortech.2016.04.093.

Tisler S, Zwiener C. 2018. Formation and occurrence of transformation products of metformin in wastewater and surface water. Sci Total Environ. 628-629:1121–1129. doi:10.1016/j.scitotenv.2018.02.105.

Trautwein C, Berset JD, Wolschke H, Kümmerer K. 2014. Occurrence of the antidiabetic drug metformin and its ultimate transformation product guanylurea in several compartments of the aquatic cycle. Environ Int. 70:203–212. doi:10.1016/j.envint.2014.05.008.

Yao Y, Xu F, Chen M, Xu Z, Zhu Z. 2010. Adsorption behavior of methylene blue on carbon nanotubes. Bioresour Technol. 101(9):3040–3046. doi:10.1016/j.biortech.2009.12.042.

Yoon K, Cho D, Tsang DCW, Bolan N, Rinklebe J, Song H. 2017. Fabrication of engineered biochar from paper mill sludge and its application into removal of arsenic and cadmium in acidic water. Bioresour Technol. 246:69–75. doi:10.1016/j.biortech.2017.07.020.

Zhao B, Nan X, Xu H, Zhang T, Ma F. 2017. Sulfate sorption on rape (*Brassica campestris* L.) straw biochar, loess soil and a biochar-soil mixture. J Environ Manage. 201:309–314. doi:10.1016/j.jenvman.2017.06.064.

Zhu S, Liu YG, Liu SB, Zeng GM, Jiang LH, Tan XF, Zhou L, Zeng W, Li TT, Yang CP. 2017. Adsorption of emerging contaminant metformin using graphene oxide. Chemosphere. 179:20–28. doi:10.1016/j.chemosphere.2017.03.071.